Journal of Structural Geology, Vol. 10, No. 4, pp. 347 to 360, 1988
Printed in Great Britain

0191-8141/88 $03.00 + 0.00

The use of asymmetric pressure shadows in mylonites to determine the sense of shear

HIDEO TAKAGI* and MAYUMI ITO†

*Institute of Earth Science, School of Education, Waseda University, Nishiwaseda, Shinjuku, Tokyo, 160 Japan, and †Fussa High School, Kitaden-en, Fussa, Tokyo, 197 Japan

(*Received* 30 *August* 1987; *accepted in revised form* 7 *January* 1988)

Abstract—Asymmetric pressure shadows (APS) on both sides of a rigid porphyroclast are commonly observed in mylonites along the Median Tectonic Line (MTL) in Japan. It is one of the most noticeable asymmetric microstructures, showing that the porphyroclasts have rotated during non-coaxial laminar flow in a ductile shear zone. The shadow domains are filled with recrystallized quartz and K-feldspar. Excepting APS, various asymmetric microstructures in the mylonites indicate a sinistral sense of displacement throughout the ductile shear zone along the MTL.

Based on the shape analysis of APS in *XZ* section (parallel to the mylonitic lineation and normal to the mylonitic foliation), the following results were obtained: (1) the relative position of the APS with respect to a porphyroclast is not a reliable criterion for deducing the sense of shear; and (2) the drag angle (β) of the shadow boundaries with respect to the mylonitic foliation in each quartered domain is diagnostic of the sense of shear; when the shearing is sinistral, β in upper right- and lower left-hand side of a porphyroclast is larger than β in upper left- and lower right-hand side, and vice versa for dextral shearing. These results demonstrate that the drag patterns of APS around porphyroclasts in mylonites are highly reliable indicators for the determination of the sense of shear.

INTRODUCTION

IN A small-scale ductile shear zone, the traces of foliations (schistosities) with respect to the zone boundaries clearly indicate the sense of shear (Ramsay & Graham 1970). In a large-scale ductile shear zone, however, except for the relationships between *C/S* and *C'/S–C* structures (cf. Berthé *et al.* 1979) it is often difficult to deduce the sense of shear from the traces of foliations. In such cases, asymmetric microstructures in sheared rocks provide useful criteria for the deduction of the sense of shear (Simpson & Schmid 1983, Lister & Snoke 1984, Hanmer 1984). Among such microstructures, asymmetric pressure shadows (APS) have been commonly used as a kinematic indicator. In previous descriptions, APS have often been illustrated in association with rotated porphyroblasts which show sigmoidal trails of inclusions which indicate clearly the sense of shear. Rotated garnets (snowball garnets) have received much attention in this respect (e.g. Rosenfeld 1970, De Wit 1976, Schoneveld 1977, Powell & Vernon 1979). On the other hand, where APS are associated with porphyroclasts or porphyroblasts without intracrystalline features to indicate the sense of shear, contradictory deductions have been made concerning the sense of shear based on the same relationship between the APS and the porphyroblast or porphyroclast (e.g. Fairbairn 1950, Stauffer 1970, Lister & Price 1978, Simpson & Schmid 1983, Faure 1985). Recently, Passchier & Simpson (1986) classified porphyroclast–tail systems in mylonitic rocks as kinematic indicators. Further theoretical and experimental studies on clast–tail systems have been made by Passchier (1987) and Van Den Driessche & Brun (1987), respectively. This article discusses the significance of APS as reliable criteria to deduce the sense of shear using a different geometric analysis from that used by Passchier & Simpson (1986). The term 'pressure shadow' in this paper excludes the 'pressure fringe' (Spry 1969) which consists of fibrous minerals adjacent to a rigid grain such as pyrite or magnetite.

SAMPLES STUDIED AND THEIR GEOLOGIC SETTING

The samples studied come from well-foliated mylonites which occur along the Median Tectonic Line (MTL) dividing two contrasting metamorphic belts, the low P/T Ryoke belt and high P/T Sambagawa belt in the Chubu and the Kinki districts of Japan (Fig. 1). The mylonites are derived from Cretaceous granitic rocks in the Ryoke belt. The samples were collected mainly from the course of the Yamamuro River in the Takato area and tributaries (Nishimitsu-zawa and Yatategi-zawa) of the Kashio River in the Kashio area, with subsidiary samples from the Urakawa area, Higashimata-dani in the Kayumi area and the southern side of Mt Kono in the Kishiwada area (Fig. 2). The geologic setting, petrography and fabrics of the mylonites in the Takato and the Kashio area have been described by Takagi (1984, 1986) and Hayashi & Takagi (1987), those in the Kayumi area by Takagi (1985), and those in the Kishiwada area by Ichihara *et al.* (1986), and is the topic of work in preparation.

Protoliths of mylonites in the Chubu district (Takato, Kashio and Urakawa area) (Fig. 1—localities 1, 2 and 3) are gneissose tonalite and granodiorite, with subordinate amounts of pelitic and quartzose metasediments

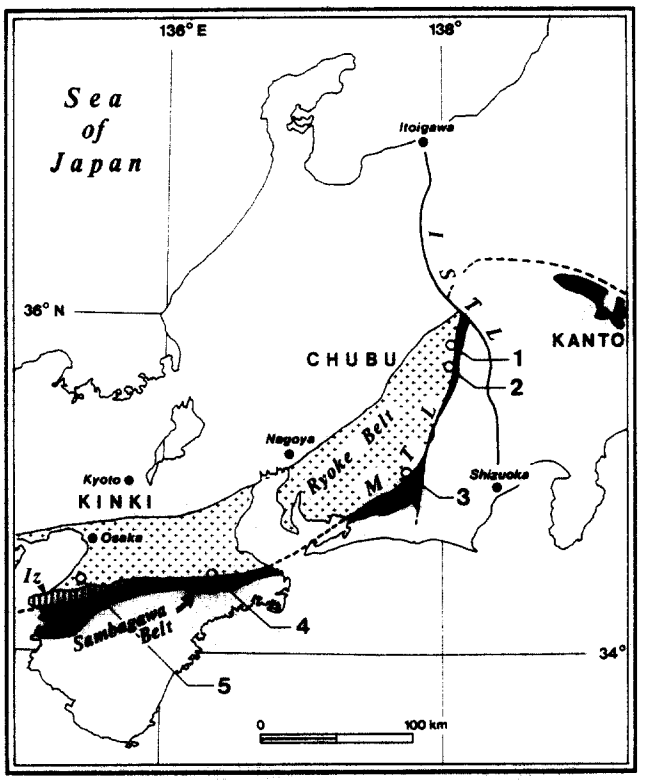

Fig. 1. Index map showing the locations of the study areas: 1. Takato, 2. Kashio, 3. Urakawa, 4. Kayumi, 5. Kishiwada. MTL: Median Tectonic Line, ISTL: Itoigawa–Shizuoka Tectonic Line, Iz: Izumi Group in the Ryoke belt.

occurring as small lenticular bodies within the granitic rocks. The mylonites are typical *L–S* tectonites characterized by mineral banding on a millimetric scale defining a mylonitic foliation (S_m) and by linear quartz aggregates on S_m defining a mylonitic lineation (L_m).

Mylonites derived from granitic rocks are composed of porphyroclasts (plagioclase, K-feldspar, ±hornblende) and recrystallized matrix minerals (quartz, biotite, K-feldspar, plagioclase, ±chlorite, ±muscovite) with accessory minerals (allanite, epidote, sphene, zircon, apatite). Reductions in grain size and in porphyroclast content are diagnostic features of mylonitic rocks compared to the adjacent parent rocks. The grain size of recrystallized quartz is one of the most sensitive indicators of the grade of mylonitization (Takagi 1984). Grain size was measured randomly on 200 grains in mylonitic rocks from the Kashio area. Figure 3(a) indicates the geometric mean ($\bar{s}$) grain size of recrystallized quartz in relation to the distance (D) from the MTL. It shows a marked grain-size reduction of recrystallized quartz grains toward the MTL. The volume per cent of porphyroclasts was determined in mylonitic rocks from the Takato and the Kashio areas. There is an overall reduction in the volume per cent of porphyroclasts toward the MTL although this is not highly pronounced (Fig. 3b).

Mylonites in the Kayumi area (Fig. 1—locality 4) originated from gneissose tonalite and quartz diorite. Pressure shadows and mineral banding are not common in these mylonitic rocks; however, APS can be observed exceptionally in an analyzed sample (MSR6) derived from gneissose granodiorite.

Mylonites in the Kishiwada area (Fig. 1—locality 5) are developed in a shear zone (inner shear zone of the Ryoke belt) about 10 km north of the MTL. They originated from gneissose granite, granodiorite and tonalite. The analyzed sample (SNR63) is ultramylonite of gneissose granite origin.

Mylonitic foliations (S_m) dip vertically or steeply NW and mylonitic lineations (L_m) are oriented nearly horizontally in all the areas investigated along the MTL. In addition to APS, asymmetric microstructures, such as displaced broken grains, orientation of spindle-shaped porphyroclasts ('fish') of mica, feldspar and hornblende, oblique quartz elongation fabrics, shear band foliations 20–30° oblique to S_m (viz. *C'/S–C* relationship) and intrafolial drag folds, are common in the mylonites. Each microstructure independently gives the same answer (sinistral) for the sense of shear throughout the ductile shear zone along the MTL. The microstructural characteristics of the mylonites mentioned above indicate that the mylonites formed during non-coaxial ductile deformation.

FABRIC OF PORPHYROCLASTS

The fabric of each of the rigid grains (porphyroclasts) was analyzed firstly on an *XZ* section normal to S_m and parallel to L_m. The axial ratio x/z and the angle α of the grain long axis x with respect to S_m were measured on 100 grains of plagioclase porphyroclasts. The relationship between α and x/z is shown in Fig. 4. α (<90°) is defined as positive when it is measured clockwise with respect to S_m. Figure 4 shows the following features: (1) where α angles are divided into four, the lower angle ($\alpha < 22.5°$) accounts for nearly 50% of grains and the higher angle ($\alpha > 67.5°$) accounts for more than 10%; (2) the porphyroclasts with higher axial ratio ($x/z > 2$) are plotted in lower α angle field; (3) the x axis tends to tilt back against the shear direction rather than to show a normal monoclinic vergence pattern. These lines of evidence suggest that the porphyroclasts floating in the recrystallized matrix minerals have rotated during ductile shear movement.

The shape of pressure shadows around a porphyroclast is schematically illustrated in Fig. 5 from the observation of three mutually perpendicular sections (*XZ*, *YZ*, *XY*). The shadow domains on both sides of a porphyroclast often extend into the matrix as ribbons parallel to mineral banding. The shape of the cross-section of the ribbons in *YZ* section is elliptical with an axial ratio (y/z) of about 2. The porphyroclasts commonly show extension cracks and are occasionally pulled apart, the open cracks being welded by a quartz fill. In *XY* section a conjugate set of cracks is commonly observed (Fig. 6), indicating extension along the *Y* direction. The features described above demonstrate that the mode of strain during mylonitization was not merely a uniaxial extension, but there was noticeable flattening into the shear plane.

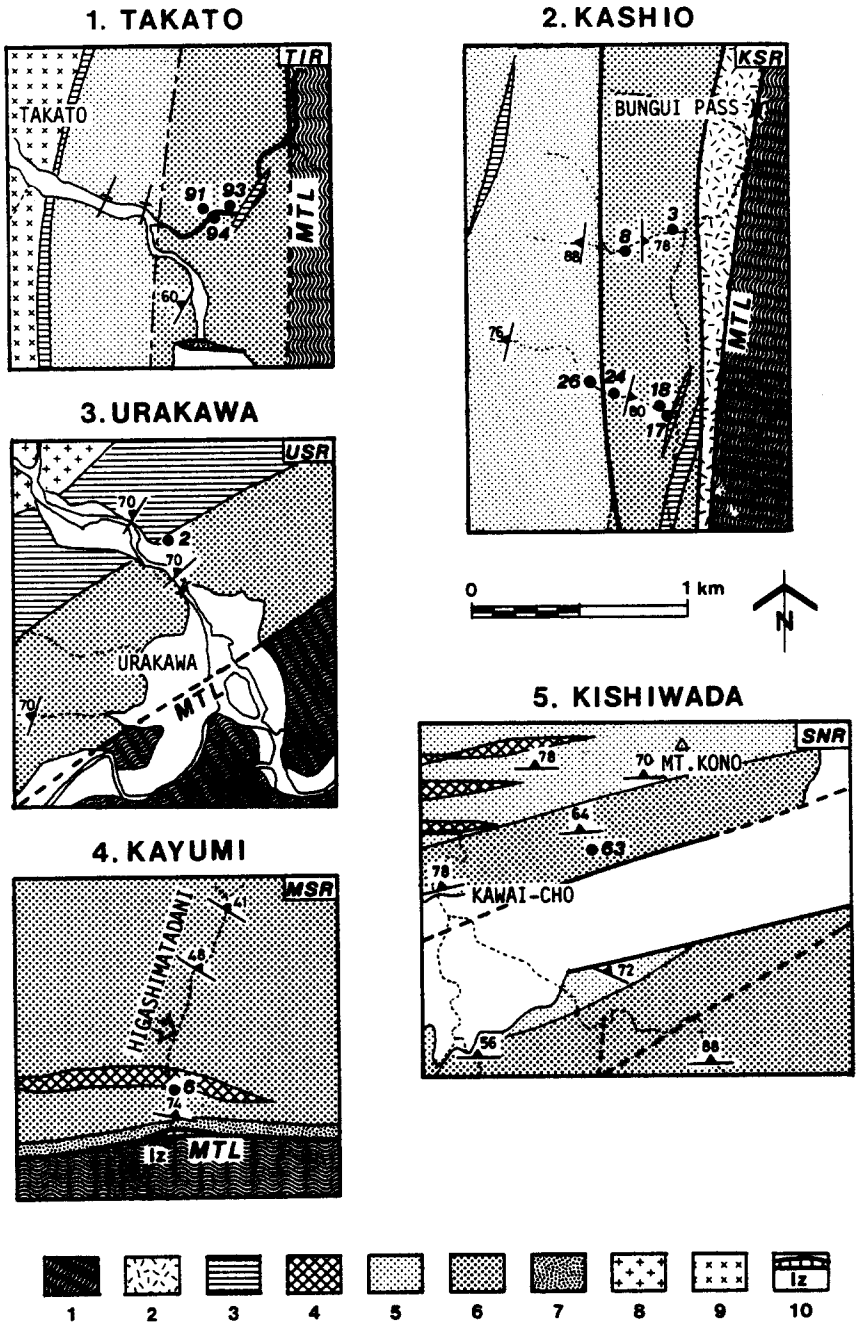

Fig. 2. Simplified geologic maps of the five areas in Fig. 1, with locations of analyzed samples. Key to lithologies: 1. Sambagawa crystalline schists, 2. microbrecciated psammitic gneiss, 3. Ryoke metamorphic rocks and phyllonites, 4. basic rocks, 5. mylonitic gneiss, 6. mylonites and blastomylonites, 7. flinty (ultra-) mylonite, 8. Tenryukyo granite, 9. Katsuma quartz diorite, 10. Cretaceous Izumi group. MTL: Median Tectonic Line.

MINERAL COMPOSITION OF APS

We can clearly observe the composition and microstructure of fine-grained polyphase aggregates by using back scattered electron (BSE) images under the electron probe microanalyzer (Jeol JXA-733). In the BSE-image, the contrast of brightness (i.e. back scattered electron coefficient) is related to the difference of the mean atomic number ($\bar{Z}$) of the mineral; the larger $\bar{Z}$, the lighter the tone. The order of decreasing brightness among the essential minerals in the granitic rocks is as follows; biotite ($\bar{Z}$ = 14.59), K-feldspar ($\bar{Z}$ = 11.85), plagioclase (e.g. $Ab_{70}An_{30}$: $\bar{Z}$ = 11.07) and quartz ($\bar{Z}$ = 10.80). Albite ($\bar{Z}$ = 10.71), which occurs as a minor secondary mineral in the matrix of mylonites, is impossible to distinguish from quartz using only the BSE-image.

The shadow domains of the APS are composed of quartz and K-feldspar with subsidiary mica minerals (Fig. 7). Quartz and K-feldspar grains are larger in size than those in the matrix. K-feldspar dominates the shadow domains where they surround a plagioclase porphyroclast, whereas the shadow domains consist of both quartz and K-feldspar where they surround a K-

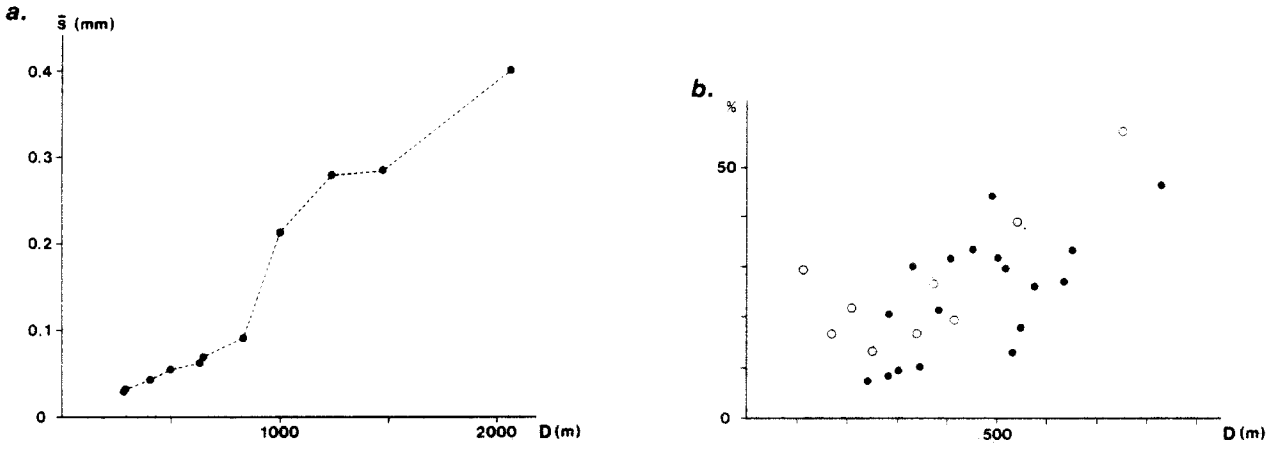

Fig. 3. (a) Relationship between the geometric mean grain size ($\bar{s}$) of recrystallized quartz and the distance (D) from the MTL in the Kashio area. (b) Relationship between the modal content of porphyroclasts and D. Open circles: Takato area, solid circles: Kashio area.

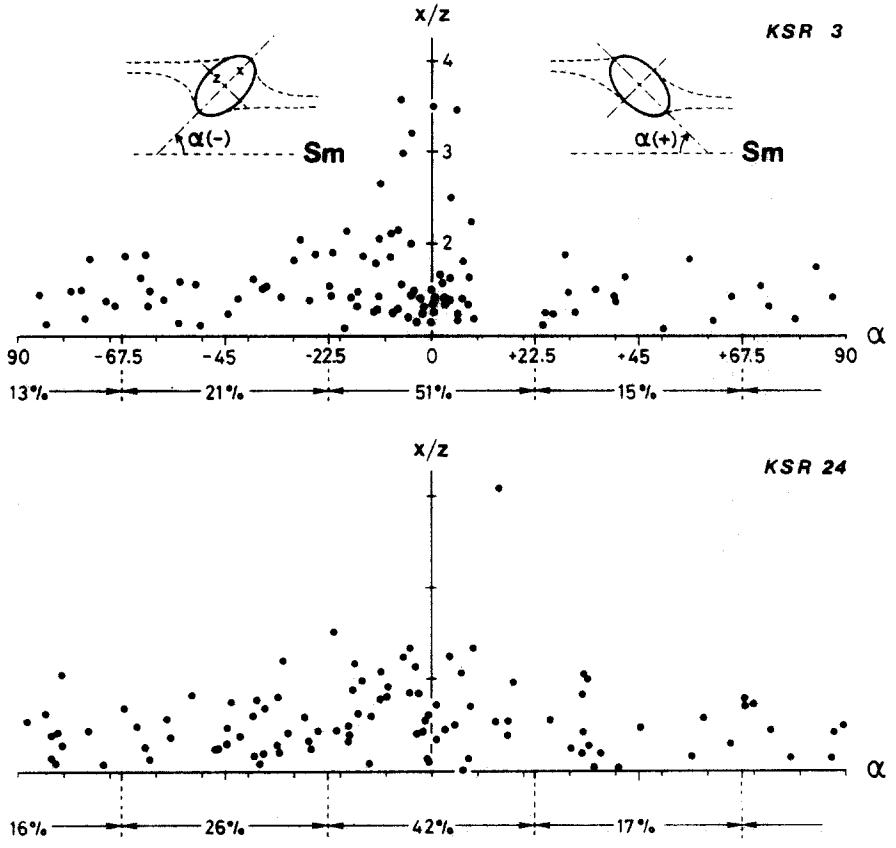

Fig. 4. Relationship between the α angle (trend of the grain long axis) and aspect ratio (x/z) of porphyroclasts in the mylonites from the Kashio area.

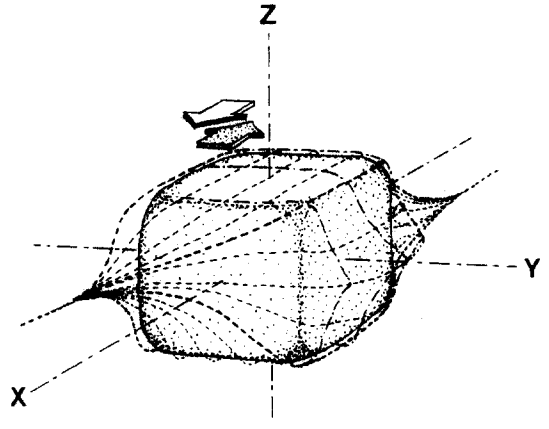

Fig. 5. Schematic illustration of APS on both sides of a porphyroclast under a sinistral sense of shear.

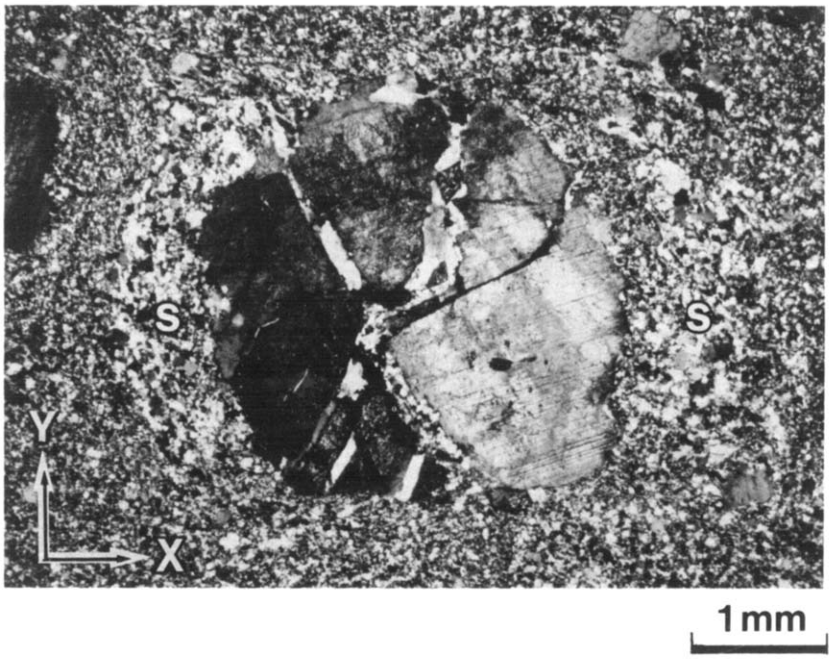

Fig. 6. Conjugate extension cracks with quartz fill in a plagioclase porphyroclast. Section (XY) parallel to S_m. s: Shadow domains, XPL (=crossed polarizers).

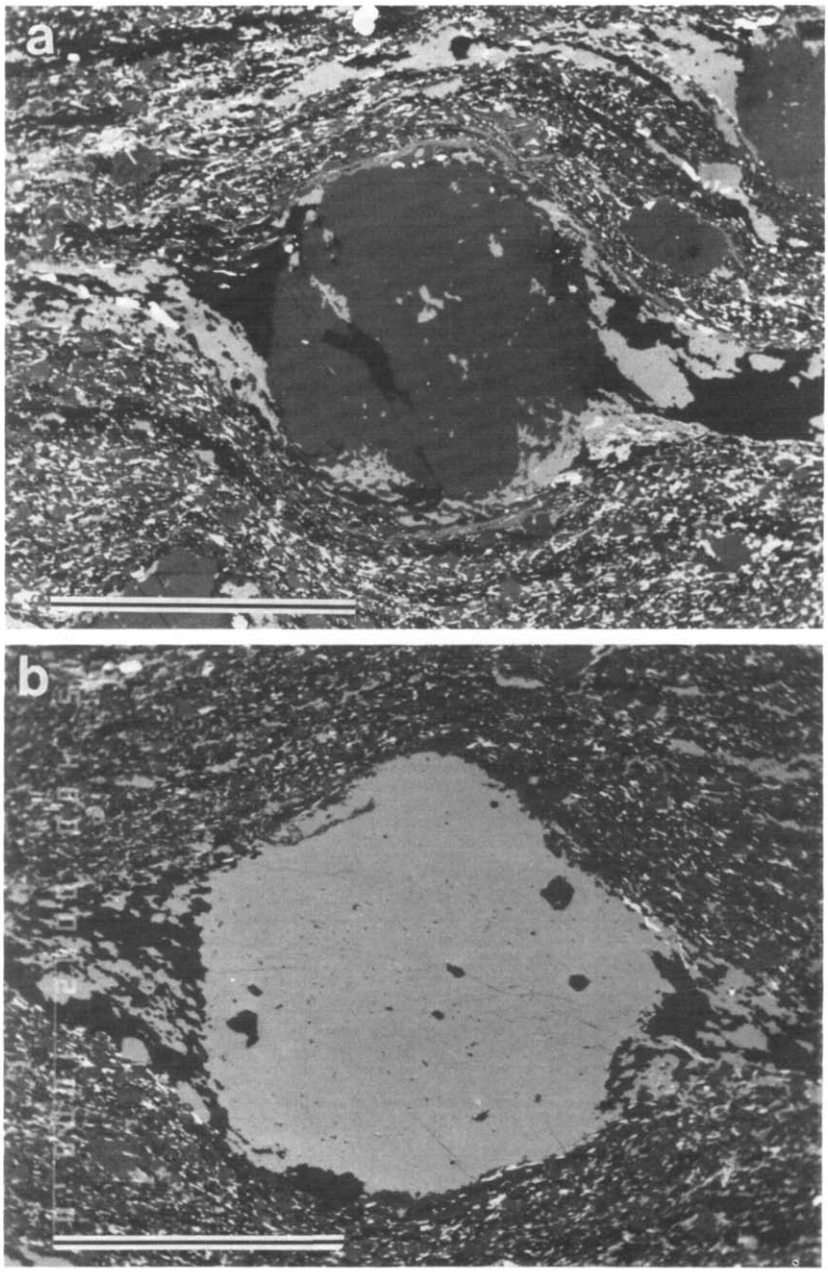

Fig. 7. BSE-image photomicrographs of APS surrounding a porphyroclast of plagioclase (a) and K-feldspar (b). Black: quartz, dark gray: plagioclase, lighter gray: K-feldspar, light: biotite and subsidiary accessory minerals. Scale bar = 1 mm.

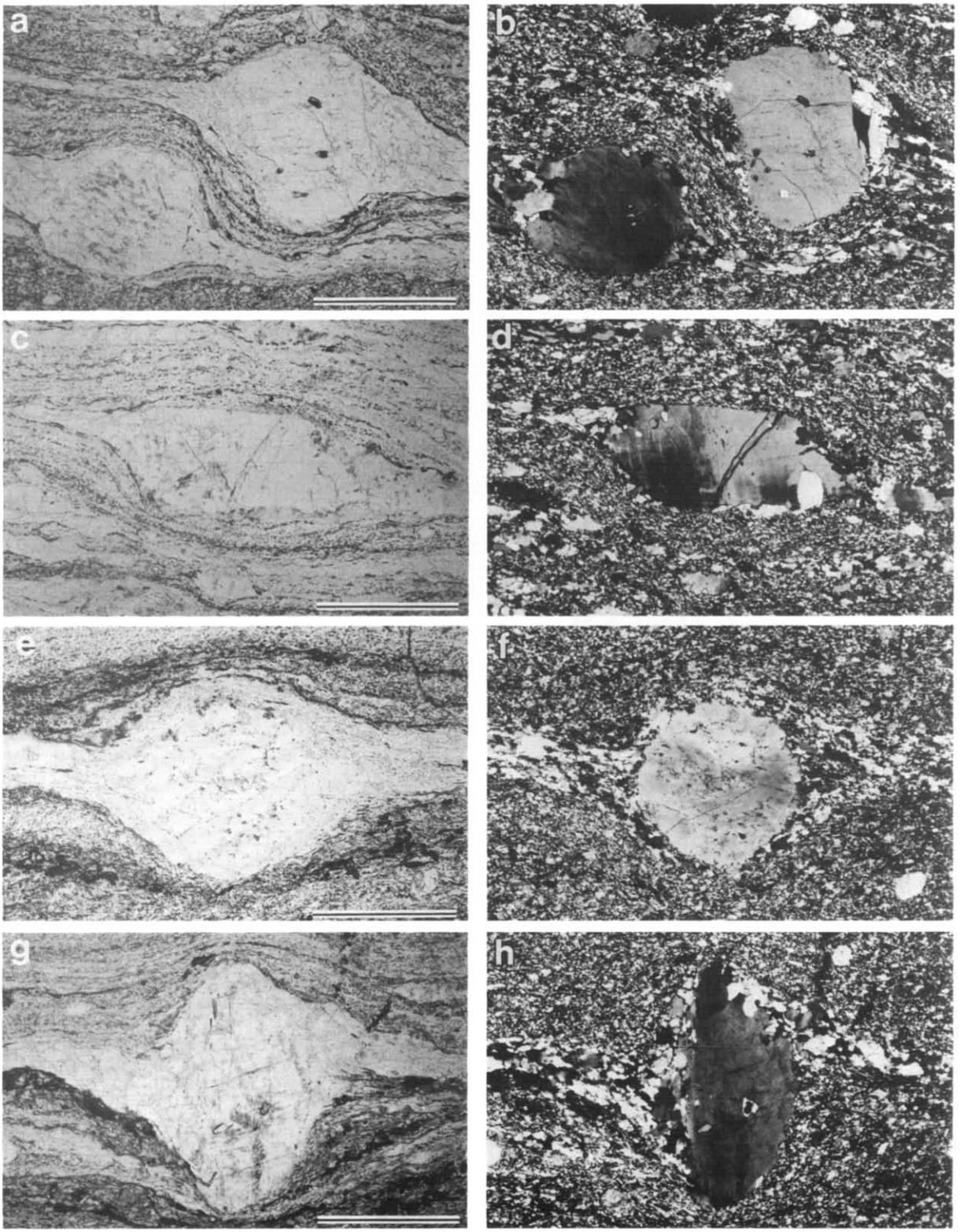

Fig. 8. Typical APS surrounding porphyroclasts of K-feldspar in the mylonites from the Kashio area. (a), (c), (e), (g): PPL (=plane polarized light), (b), (d), (f), (h): XPL, scale bar = 1 mm.

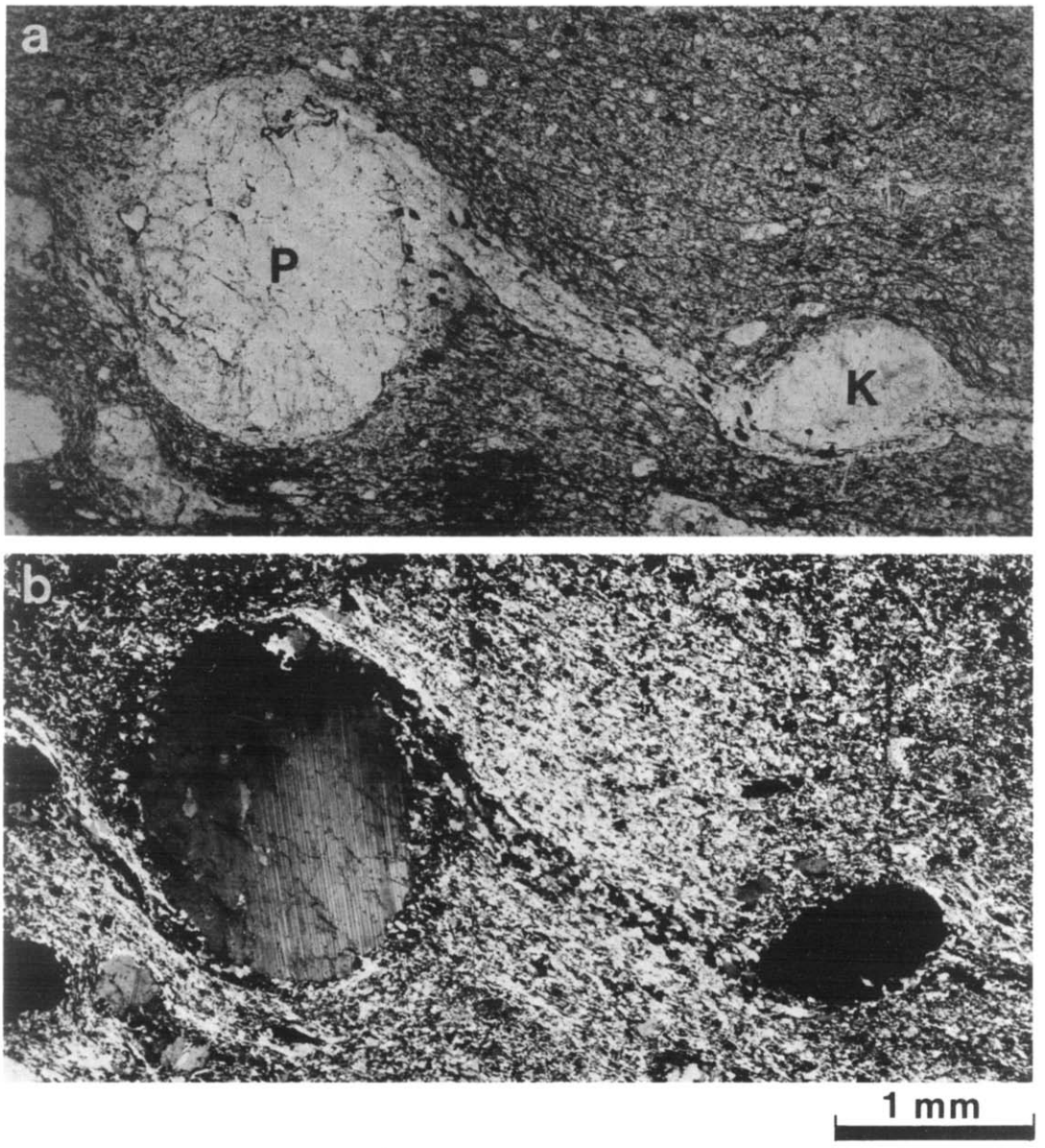

Fig. 9. Stretched APS connecting two porphyroclasts which clearly exhibits rotation of the porphyroclasts during mylonitization. P: Plagioclase, K: K-feldspar, (a) PPL, (b) XPL.

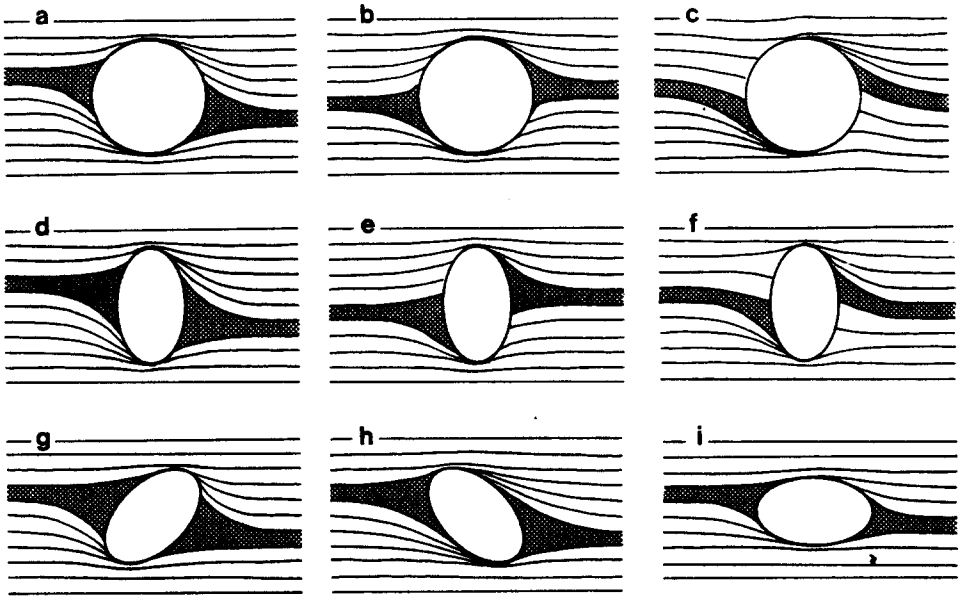

Fig. 10. Schematic illustrations of various types and positions of APS with respect to the porphyroclasts.

feldspar porphyroclast. This compositional evidence of the APS suggests that the majority of the APS mineral filling is not dynamically recrystallized material of the host grain and/or reaction softened material constituting tails (Passchier & Simpson 1986) but comes dominantly from the rock matrix. Furthermore the following compositional asymmetry can be observed: K-feldspar tends to occupy the upper right-hand and lower left-hand sides relative to the positioning of quartz in the same shadow domain (Fig. 7a). It is one of the more notable examples of stress-induced mineral differentiation in metamorphic tectonites and will be discussed in a separate paper.

POSITIONING OF APS WITH RESPECT TO PORPHYROCLAST

Based on the observation of outcrops, thin sections under the microscope (Fig. 8), and BSE-images under the EPMA (Fig. 7), various shapes of pressure shadows occur, as well as a variety of shapes and fabrics of the porphyroclasts. These variations are schematically illustrated in Fig. 10. The mylonites also contain stretched pressure shadows connecting two porphyroclasts (Fig. 9). This example clearly demonstrates that the rotation of the porphyroclasts continued after the formation of the associated pressure shadows.

To clarify the asymmetry of pressure shadows, the positioning with respect to a porphyroclast was examined. The positioning of the pressure shadows is classified geometrically into three types (Fig. 11); type I shadow domains at the upper left-hand and lower right-hand side of the porphyroclast, type II at symmetric positions in relation to the porphyroclast and type III at the upper right-hand and lower left-hand side of the porphyroclast.

Examples of the type I are shown in Figs. 7(a) and 8(a–d), type II in Figs. 7(b) and 8(e & f) and type III in Figs. 8(g & h) and 9. The frequency of each type was measured on 40 porphyroclasts in each section of the three samples from the Kashio area. Type I accounts for nearly half, type II for 30% and type III for 20% of the porphyroclasts in these samples (Fig. 11). Consequently, by using the position of pressure shadow domains with respect to a porphyroclast only, we cannot satisfactorily determine the sense of shear.

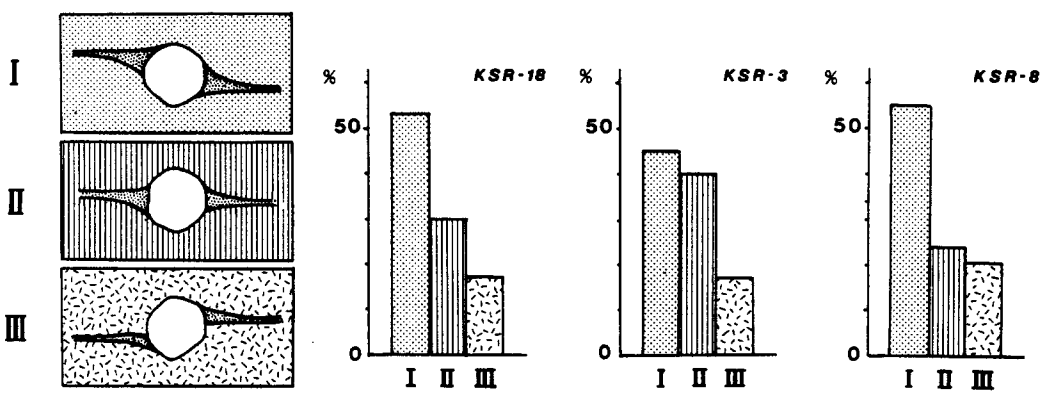

Fig. 11. The frequency of the three types (I, II, III) divided on the basis of the positioning of APS with respect to a porphyroclast in the three samples.

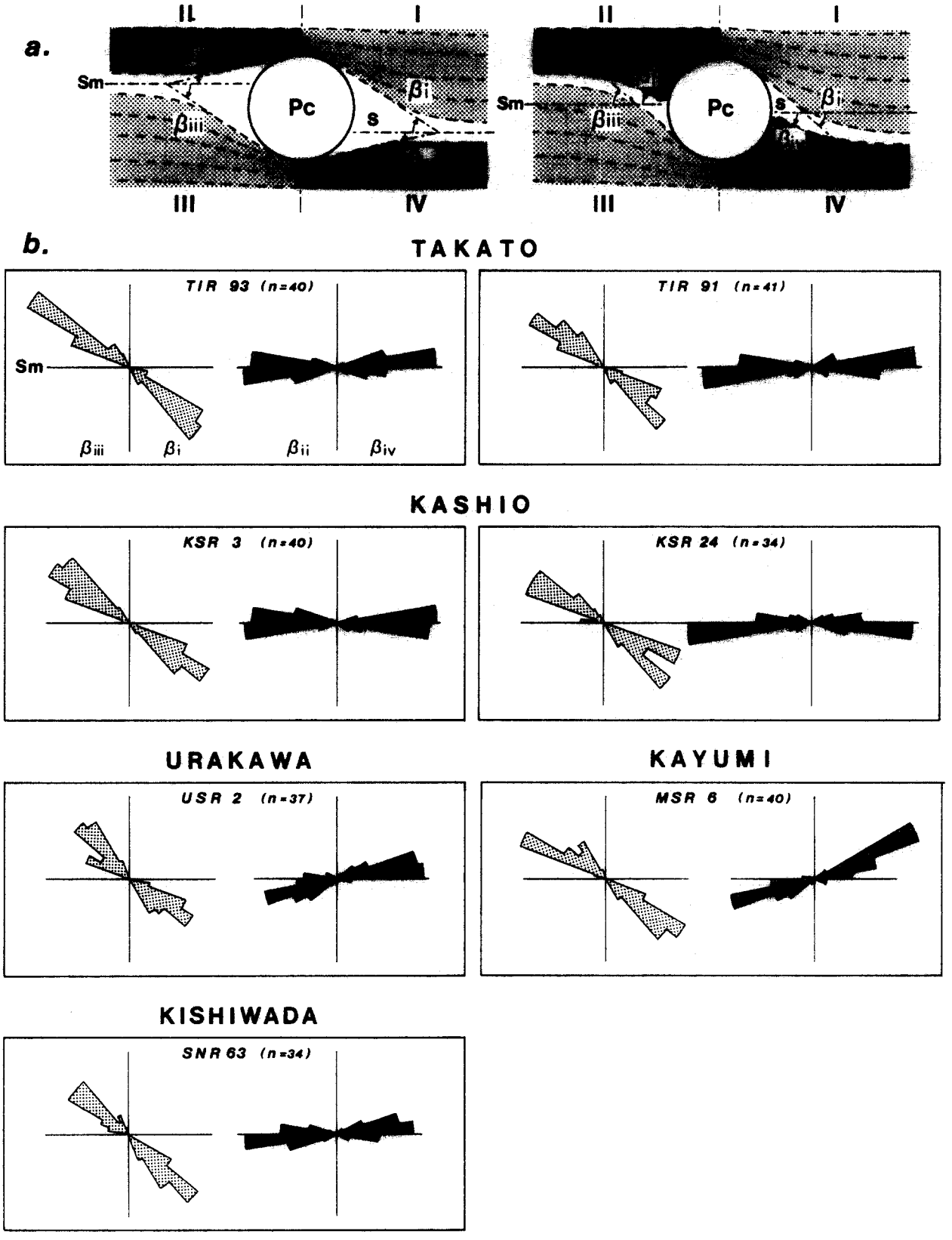

Fig. 12. (a) Definition of drag angles (β_i, β_{ii}, β_{iii}, β_{iv}) in quartered domains around a porphyroclast (Pc). s: Shadow domains. (b) Rose diagrams showing the frequency distributions of the drag angles in each sample.

DRAG ANGLES OF PRESSURE SHADOWS AROUND PORPHYROCLASTS

It is a common characteristic of APS in the mylonites along the MTL that the angle between the boundary of a shadow domain against the matrix and S_m is larger in the upper right- /lower left-hand sides than in lower right- /upper left-hand sides of a porphyroclast. This angle is defined as the drag angle (β) which is positive when it is measured in a clockwise direction from S_m and negative when measured in an anticlockwise direction. Four domains (I, II, III, IV) are divided by the geometric axis of a porphyroclast normal to S_m and the margin of the shadow domains (Fig. 12a). Drag angles ($\beta_i, \beta_{ii}, \beta_{iii}, \beta_{iv}$) were measured in each domain (I, II, III, IV, respectively) on nearly 40 porphyroclasts in each sample from the five areas of study. The frequency distributions of β at 10° intervals are shown in rose diagrams (Fig. 12b). The distribution patterns of the drag angles clearly indicate the monoclinic symmetry of the movement pattern. The drag angles are not influenced by variations in the axial ratio nor by the α value of the porphyroclasts.

The relationships of the drag angles of pressure shadows on the same side of the porphyroclasts (i.e. β_{ii} and β_{iii}, β_i and β_{iv}) are shown in Fig. 13. The broken lines indicate the traces of $\beta_{ii} = -\beta_{iii}$ and $\beta_i = -\beta_{iv}$, in which both sides of the shadow domains are symmetric. The greater the distance from this line, the more asymmetric the pressure shadow. Therefore the distance from this line is defined as the asymmetric index (A),

$$A = \frac{1}{\sqrt{2}}\left(\frac{\beta_{ii} + \beta_{iii}}{2} + \frac{\beta_i + \beta_{iv}}{2}\right).$$

The broken lines in Fig. 13 correspond to $A = 0$. Almost all of the drag angles in the mylonites are plotted in the positive ($A > 0$) field (Fig. 13). These results mean that most of the APS exhibit the same sense (sinistral) of shear as is given by other asymmetric microstructures which may be used as kinematic indicators.

The asymmetry index (A) was measured on nearly 40 porphyroclasts in each sample and the mean value ($\bar{A}$) and standard deviation σ are listed in Table 1 together with the following parameters; the distance (D) from the MTL, modal content of the porphyroclasts and the maximum grain size (s_{max}) of recrystallized quartz. There is no relationship between $\bar{A}$ and s_{max} (i.e. the grade of mylonitization). On the other hand, there is a correlation between the standard deviation (σ) and the porphyroclast content (Table 1), probably because mutual interference among the porphyroclasts occurs when the porphyroclast content is large. The mean asymmetry index $\bar{A}$ of the mylonite from the Kayumi area is somewhat smaller than that from other areas, it probably relates to the poor development of mylonitic lineation and of APS, and widespread (3–5 km from the MTL) grain-size reduction of recrystallized quartz in the Kayumi area suggesting a higher angle between the geometrical trend of the shear zone and the maximum compressive stress axes (Takagi 1985).

DISCUSSION

Based on the shape and long-axis orientation of the porphyroclasts and on the pattern of the APS, the porphyroclasts must have rotated differentially during the laminar flow of the ductile matrix in the mylonites. The period of precipitation of quartz and K-feldspar was probably prolonged in the domains of stress relaxation associated with drag caused by rotation of porphyroclasts.

The rotation of a rigid grain in a ductile matrix has been simulated by two-dimensional shear box experiments (Ghosh 1975, Ghosh & Ramberg 1976, Passchier & Simpson 1986, Van Den Driessche & Brun 1987). They used viscous silicone putty to represent the ductile matrix material and a rigid object for simulating a rolling clast.

Ghosh (1975) indicated that where the pre-existing foliation (shown by marker lines) is initially at a high angle to the direction of simple shear, different senses of drag pattern can occur around a rigid grain, and where the pre-existing foliation is initially parallel to the direction of simple shear, the same sense of drag pattern occurs all over the contact. Outside the shear zone, original compositional banding of the protoliths is nearly parallel to S_m in the mylonites along the MTL in the Chubu (Takagi 1986) and the Kinki (Takagi 1985) dis-

Table 1. The mean asymmetric index ($\bar{A}$) of APS and its standard deviation (σ) together with the distance from the MTL (D), maximum size (s_{max}) of recrystallized quartz and modal content of porphyroclastic minerals in each sample from the five investigated areas

Area	Sample No.	D (m)	s_{max} (mm)	Total:	Mode (%) of porphyroclasts Pl	Kf	Hb	etc.	$\bar{A}$	σ
Takato	TIR93	250	0.08	13.2:	8.6	1.2	3.4	0	25.2	10.6
	TIR94	340	0.10	17.3:	14.6	0.3	2.4	0	23.6	6.0
	TIR91	415	0.11	19.5:	15.3	4.3	0	0	26.0	9.8
Kashio	KSR17	240	0.08	7.5:	4.9	0.9	1.6	0.1	30.9	6.6
	KSR18	280	0.09	8.3:	6.6	1.7	0	0	21.3	9.3
	KSR3	345	0.12	11.0:	9.5	1.0	0	0.5	26.5	7.4
	KSR8	530	0.25	13.2:	11.0	2.1	0	0.1	18.1	10.4
	KSR24	545	0.20	18.0:	16.2	1.7	0	0.1	23.4	10.8
	KSR26	630	0.60	26.9:	25.6	1.3	0	0	29.7	11.7
Urakawa	USR2	620	0.09	19.9:	17.0	2.8	0	0.1	18.8	10.4
Kayumi	MSR6	250	0.08	28.9:	28.9	0	0	0	15.6	10.2
Kishiwada	SNR63	(10 km)	0.10	23.0:	9.2	3.7	0	0.1	27.9	10.6

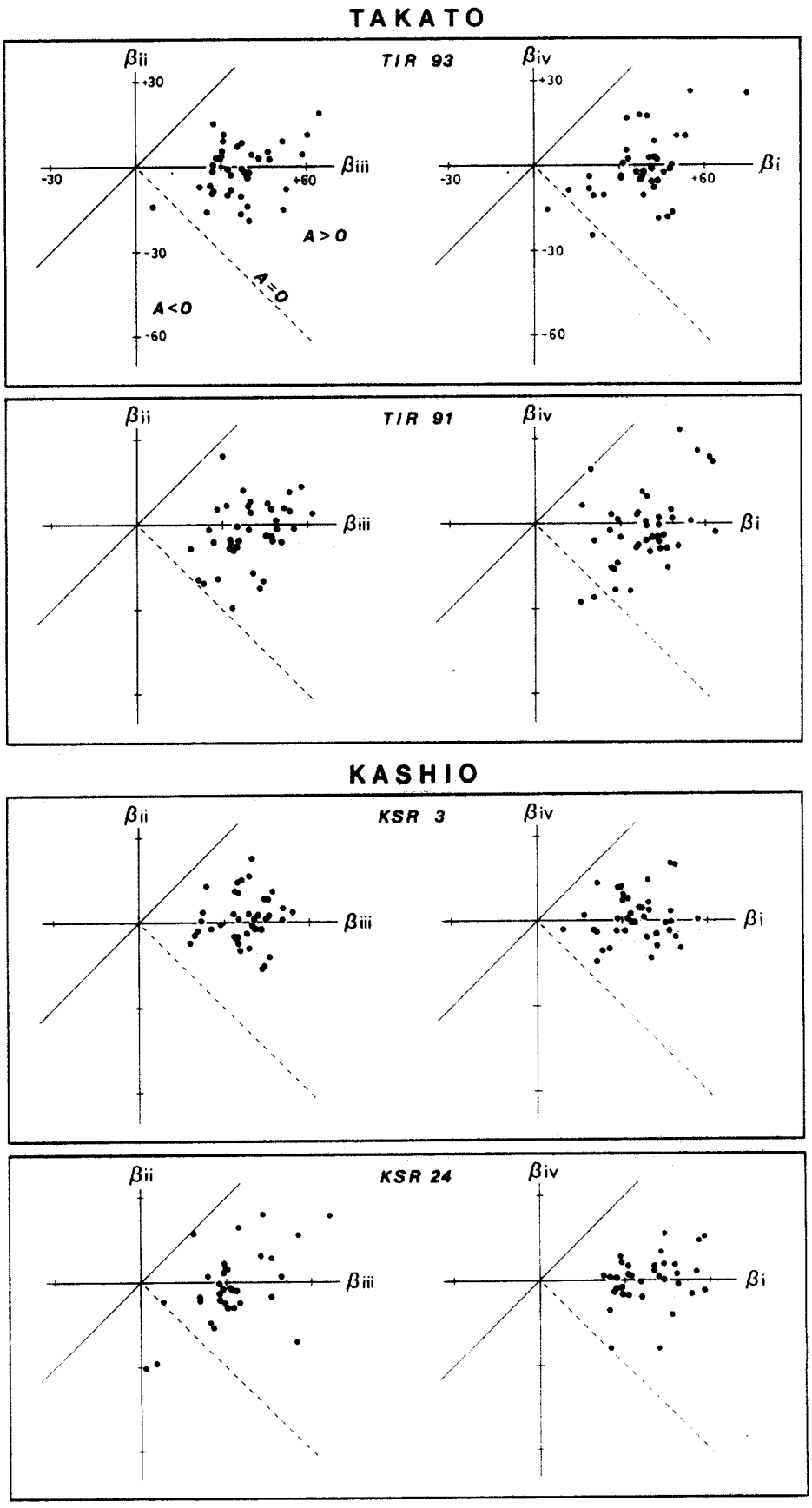

Fig. 13. Plots showing the relationships between the drag angles at the same domain of each pressure shadow (i.e. β_{ii} and β_{iii}, β_i and β_{iv}).

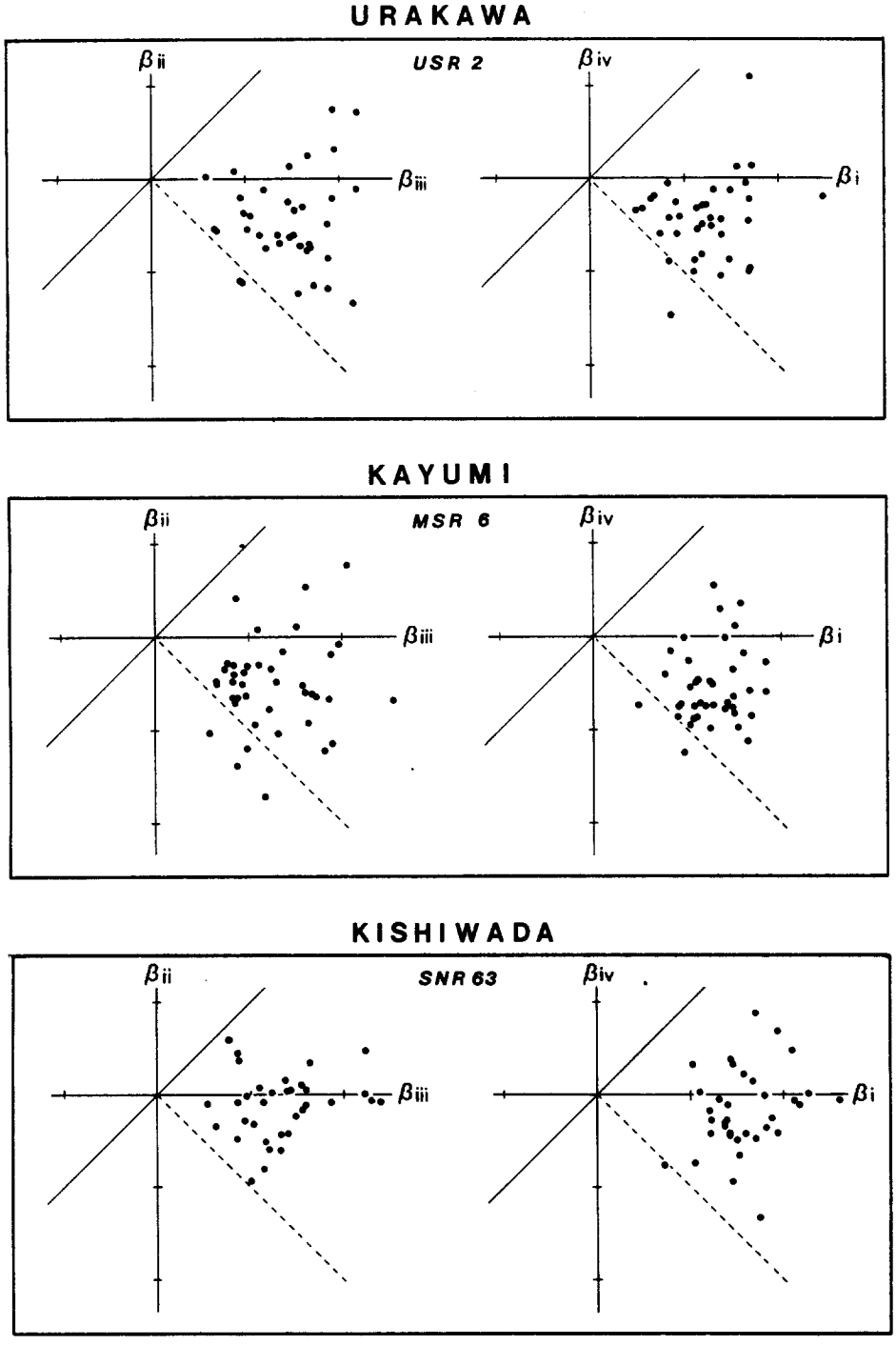

Fig. 13 *continued*.

tricts; therefore the latter case of Ghosh's results mentioned above is applicable to them.

Passchier & Simpson (1986) made various geometrical types of porphyroclast systems by shear box experiments and they concluded that the formation of various types of systems were related to recrystallization rate ($\dot{R}$) with respect to the rate of deformation ($\dot{r}$). According to their results, at high $\dot{R}/\dot{r}$ values, wedge-shaped 'σ_a type' (e.g. Figs. 10a, d, g, h & i in this paper) develop, whereas 'δ type' (e.g. Figs. 10 c & f) only develop at high shear strain values. Both types mentioned above coexist in the same sample from the Takato and the Kashio area. This is probably due to microstructural and mineralogical inhomogeneities such as the distribution pattern of different minerals and of different grain-sized particles in the mylonites. The shape of 'σ_b type' porphyroclast systems according to Passchier & Simpson (1986) is highly controlled by another structural element (shear band foliation) and thus this type was excluded for investigation in this paper. Based on the geometric analysis together with the shear box experiments previously studied, the 'drag angles method' presented in this paper enables the shear sense determination without any ambiguity whether the microstructure is a clast–

pressure shadow system or clast–tail system, or whether the system is of σ_a or δ type (cf. Van Den Driessche & Brun 1987).

Acknowledgements—The authors would like to express sincere thanks to Dr A. J. Barber of London University for critical reading of the manuscript and for correcting the English. We also acknowledge H. Nagahama, H. Osawa and K. Hiro-oka for providing analyzed thin sections.

REFERENCES

Berthé, D., Choukroune, P. & Jegouzo, P. 1979. Orthogneiss, mylonite and non coaxial deformation of granites: the example of the South Armorican Shear Zone. *J. Struct. Geol.* **1**, 31–42.

De Wit, M. J. 1976. Metamorphic textures and deformation: A new mechanism for the development of syntectonic porphyroblasts and its implications for interpreting timing relationships in metamorphic rocks. *Geol. J.* **11**, 71–100.

Fairbairn, H. W. 1950. Pressure shadows and relative movements in a shear zone. *Trans. Am. Geophys. Union* **31**, 914–916.

Faure, M. 1985. Microtectonic evidence for eastward ductile shear in the Jurassic orogen of SW Japan. *J. Struct. Geol.* **7**, 175–186.

Ghosh, S. K. 1975. Distortion of planar structures around rigid spherical bodies. *Tectonophysics* **28**, 185–208.

Ghosh, S. K. & Ramberg, H. 1976. Reorientation of inclusions by combination of pure shear and simple shear. *Tectonophysics* **34**, 1–70.

Hanmer, S. K. 1984. The potential use of planar and elliptical structures as indicators of strain regime and kinematics of tectonic flow. *Geol. Surv. Can. Paper* **84-1b**, 133–142.

Hayashi, M. & Takagi, H. 1987. Shape fabric of recrystallized quartz in the mylonites along the Median Tectonic Line, southern Nagano Prefecture. *J. geol. Soc. Japan* **93**, 349–359.*

Ichihara, M., Ichikawa, K. & Yamada, N. 1986. *Geology of the Kishiwada District.* Quadrangle Series, scale 1 : 50,000. Geol. Surv. Japan, 1–148.*

Lister, G. S. & Price, G. P. 1978. Fabric development in a quartz-feldspar mylonite. *Tectonophysics* **49**, 37–78.

Lister, G. S. & Snoke, A. W. 1984. S–C mylonites. *J. Struct. Geol.* **6**, 617–638.

Passchier, C. W. 1987. Stable positions of rigid objects in non-coaxial flow—a study in vorticity analysis. *J. Struct. Geol.* **9**, 679–690.

Passchier, C. W. & Simpson, C. 1986. Porphyroclast systems as kinematic indicators. *J. Struct. Geol.* **8**, 831–843.

Powell, C. McA. & Vernon, R. H. 1979. Growth and rotation history of garnet porphyroblasts with inclusion spirals in a Karakoram schist. *Tectonophysics* **54**, 25–43.

Ramsay, J. G. & Graham, R. H. 1970. Strain variation in shear belts. *Can. J. Earth Sci.* **7**, 786–813.

Rosenfeld, J. L. 1970. Rotated garnets in metamorphic rocks. *Spec. Pap. geol. Soc. Am.* **129**.

Schoneveld, C. 1977. A study of some typical inclusion patterns in strongly paracrystalline-rotated garnets. *Tectonophysics* **39**, 453–471.

Simpson, C. & Schmid, S. M. 1983. An evaluation of criteria to deduce the sense of movement in sheared rocks. *Bull. geol. Soc. Am.* **94**, 1281–1288.

Spry, A. 1969. *Metamorphic Textures.* Pergamon Press, Oxford.

Stauffer, M. R. 1970. Deformation textures in tectonites. *Can. J. Earth Sci.* **7**, 498–511.

Takagi, H. 1984. Mylonitic rocks along the Median Tectonic Line in Takato-Ichinose area, Nagano Prefecture. *J. geol. Soc. Japan* **90**, 81–100.*

Takagi, H. 1985. Mylonitic rocks of the Ryoke belt in the Kayumi area, eastern part of the Kii Peninsula. *J. geol. Soc. Japan* **91**, 637–651.*

Takagi, H. 1986. Implications of mylonitic microstructures for the geotectonic evolution of the Median Tectonic Line, central Japan. *J. Struct. Geol.* **8**, 3–14.

Van Den Driessche, J. & Brun, J.-P. 1987. Rolling structures at large shear strain. *J. Struct. Geol.* **9**, 691–704.

*In Japanese with English abstract.